

Braiding of anyonic quasiparticles in charge transfer statistics of a symmetric fractional edge-state Mach-Zehnder interferometer

Vadim V. Ponomarenko

Center of Physics, University of Minho, Campus Gualtar, 4710-057 Braga, Portugal

Dmitri V. Averin

Department of Physics and Astronomy, University of Stony Brook–SUNY, Stony Brook, New York 11794, USA

(Received 18 April 2010; published 9 November 2010)

We have studied the zero-temperature statistics of the charge transfer between the two edges of Quantum Hall liquids of, in general, different filling factors, $\nu_{0,1}=1/(2m_{0,1}+1)$, with $m_0 \geq m_1 \geq 0$, forming Mach-Zehnder interferometer. Expression for the cumulant generating function in the large-time limit is obtained for symmetric interferometer with equal propagation times along the two edges between the contacts and time-independent bias voltage. The low-voltage limit of the generating function can be interpreted in terms of the regular Poisson process of electron tunneling, while its leading large-voltage asymptotics is proven to coincide with the solution of kinetic equation describing quasiparticle transitions between the m states of the interferometer with different effective flux through it, where $m \equiv 1+m_0+m_1$. For $m > 1$, this dynamics reflects both the fractional charge e/m and the fractional statistical angle π/m of the tunneling quasiparticles. Explicit expressions for the second (shot noise) and third cumulants are obtained, and their voltage dependence is analyzed.

DOI: [10.1103/PhysRevB.82.205411](https://doi.org/10.1103/PhysRevB.82.205411)

PACS number(s): 73.43.Jn, 71.10.Pm, 73.23.Ad

I. INTRODUCTION

Electronic Mach-Zehnder interferometer (MZI) (Refs. 1–3) can be realized with the edge states of the Quantum Hall liquids (QHLs). Together with the quantum antidots,^{4,5} MZIs in the regime of the fractional Quantum Hall effect (FQHE) are expected^{6–8} to be useful for observation of the fractional statistics of FQHE quasiparticles. In contrast to fractional quasiparticle charge, which has been confirmed in several experiments,^{4,9,10} there is no commonly accepted observation of anyonic statistics of the quasiparticles, which remains a challenging experimental problem. Currently, this problem attracts interest in the context of solid-state quantum computation, since individual manipulation of anyonic quasiparticles involving their braiding provides an interesting possible basis for implementation of the quantum information processing.^{11–13} However, in a typical interferometer-based experimental setup, the quasiparticles emerge as a continuum of gapless edge excitations that should be described by a 1D field theory.¹⁴ Individual quasiparticles can be realized in this theory only asymptotically in a special limit. In the fractional edge-states MZI, such a limit occurs at *large* voltages, when the system is characterized by the Hamiltonian dual to the Hamiltonian of the initial electron tunneling model of the MZI. The latter is perturbative in electron tunneling at low voltages, and is much better defined, since weak electron tunneling is probably the most basic process in solid-state physics.

Several different models of the quasiparticles transport in the MZI (cf. Refs. 7, 15, and 16) were obtained from qualitative physical considerations of tunneling geometry of the interferometer. They produce conflicting result, e.g., different periods of the tunnel current modulation by the magnetic flux Φ_{ex} through the MZI. The dual description derived quantitatively from the electronic model by the instanton technique^{8,17} gives the definite model of the quasiparticle

tunneling, the main elements of which have been found previously¹⁸ for the Fabry-Perot interferometers formed by the edges with different filling factors. In this model, in agreement with the theoretical picture postulated in Ref. 7, MZI acquires $m=m_0+m_1+1$ different quantum states which differ by the effective flux Φ through it. This flux contains, in addition to the external flux Φ_{ex} , a statistical contribution, because of which the tunneling of each quasiparticle changes the effective flux by $\pm\Phi_0$, where $\Phi_0=h/e$ is the “electron flux quantum,” switching the MZI from one flux state into another. Since quasiparticle also carries the charge e/m , the change in flux by $\pm\Phi_0$ results in the change in the interference phase for the quasiparticles by $2\pi/m$ and the corresponding change in the rate of coherent tunneling through the interferometer. Summation over the m flux states in calculation of the physical quantities restores the Φ_0 periodicity of their Φ_{ex} dependence. At low voltages, this periodicity is guaranteed by the Φ_0 periodicity of the total electron tunneling amplitude.

In this work, we follow the approach to the MZI that allows us to obtain the uniform description of its transport properties in both regimes of electron and quasiparticle tunneling. We consider the standard MZI geometry (Fig. 1) with two tunneling contacts between the two effectively parallel edges of QHLs, but allow for, in general, different filling factors, $\nu_{0,1}=1/(2m_{0,1}+1)$, with $m_0 \geq m_1 \geq 0$, of these edges. The tunnel contacts between edges with different filling factors can be realized experimentally, e.g., through the gate-induced modulation of electron density in different areas of the 2D electron gas.¹⁹ In the symmetric case of equal propagation times along the two edges between the contacts, the corresponding 1D field theory permits an exact Bethe ansatz solution.⁸ Making use of this solution, we calculate the zero-temperature full counting statistics²⁰ of the charge transferred between the two edges forming the MZI. The transferred charge distribution is shown to reflect the anyonic braiding

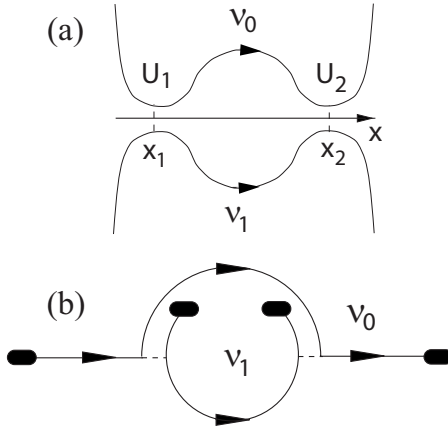


FIG. 1. Mach-Zehnder interferometer considered in this work. (a) Conceptual diagram of the two copropagating edges of QHs with different filling factors ν_0 and ν_1 coupled at points x_j , $j=1,2$, by two point contacts with tunneling amplitudes U_j . The edges are assumed to support one bosonic mode each with arrows indicating direction of propagation of these modes. (b) Schematic geometry of the edge propagation in the experimentally realized interferometers. Filled areas denote the Ohmic contacts which emit/absorb edge modes and special arrangement of which makes it possible to implement tunneling between the copropagating edges within one plane of the two-dimensional electron gas.

statistics of the tunneling quasiparticles, and splitting of electrons into quasiparticles with increasing voltage.

The paper is organized as follows. In Sec. II we introduce the model of symmetric MZI and its Bethe ansatz solution. In Sec. III, we use this solution to derive the general expression for the generating function $P(\xi)$ of the distribution of the transferred charge. The method employed in this calculation generalizes to the MZI transport through two point contacts the method developed earlier by Saleur and Weiss²¹ for a single point contact. The charge transfer statistics found for one contact²¹ demonstrated fractionalization of electron charges with increasing bias voltage across the contact. In the case of MZI, one can expect that in addition to the charge fractionalization, braiding properties of anyonic quasiparticles should emerge in the charge transfer statistics. To see this, we analyze our result for the transfer statistics in different regimes. We find that the logarithm of the cumulant-generating function separates into two parts, which for very different absolute values of the electron tunneling amplitudes in the two contacts, $U_2/U_1 \gg 1$, become identical with the cumulant-generating functions of the two separate contacts. In general, however, each “single-contact” term accounts also for the interference between the contacts. At low voltages, these single-contact terms are combined in such a way that the charge transfer occurs only in units of electron charge, with the low-voltage asymptotic describing the regular Poisson distribution of tunneling electrons. In Sec. IV, we develop analogous qualitative interpretation of the large-voltage asymptotics of the Bethe ansatz result for the generating function. The interpretation is based on the m -state model of the quasiparticle tunneling described above. Following the method of Ref. 25, the cumulant-generating function is calculated from the kinetic equation governing the

quasiparticle transitions in the basis of the m flux states. Direct comparison of this generating function with the leading asymptotics of the Bethe ansatz result reveals their coincidence under a special choice of m quasiparticle interference phases which are found as $\phi_l = [\kappa + (m-1)\pi + 2\pi l]/m$, where $l=0, \dots, m-1$ numbers the flux states of the interferometer. The l -dependent, statistical part of these phases agrees with the expected anyonic statistics of the quasiparticles, while the common phase is given by the electron interference phase κ with an additional phase shift π/m for even m . The equivalence of the two distributions in the large-voltage limit proves that the Bethe ansatz construction we implemented indeed describes the statistical transmutation of the effective flux through the MZI. In Sec. V, we use the obtained generating function to find the first three cumulants of the transferred charge distribution. We study, in particular, the voltage dependence of the first and the second cumulants proportional to the average current and the shot noise, respectively. The ratio of the two, the Fano factor, is an experimentally observable^{9,10} characteristics of the electron-quasiparticles decomposition. Finally, we consider the third cumulant, which determines the asymmetry of the transferred charge distribution around the average. In Sec. VI, we look at the special case $m=2$ which allows to obtain these cumulants in terms of the elementary functions for arbitrary voltages. The results of this work are summarized in the Conclusion.

II. MODEL OF THE SYMMETRIC MACH-ZEHNDER INTERFEROMETER AND ITS BETHE-ANSATZ SOLUTION

We start our discussion with the electronic model of the MZI (Fig. 1) formed by two single-mode edges with filling factors $\nu_l = 1/(2m_l + 1)$, $l=0,1$. Electron operator ψ_l of the edge l is expressed using the standard bosonization approach¹⁴ as

$$\psi_l = (D/2\pi\nu_l)^{1/2} \xi_l e^{i[\phi_l(x,t)/\sqrt{\nu_l} + k_l x]}.$$

Here ϕ_l are the two chiral bosonic modes propagating with velocities v_l in the same direction (to the right in Fig. 1), which satisfy the usual equal-time commutation relations $[\phi_l(x), \phi_p(0)] = i\pi \text{sgn}(x) \delta_{lp}$. The Majorana fermions ξ_l account for the mutual statistics of electrons in different edges, and D is a common energy cutoff of the edge modes. The Fermi momenta k_l correspond to the average electron density in the edges, while the operators of the density fluctuations are: $\rho_l(x, \tau) = (\sqrt{\nu_l}/2\pi) \partial_x \phi_l(x, \tau)$.

In the symmetric case of equal times of excitation propagation the contacts along the two edges and equal velocities $v_1 = v_2 \equiv v$, the two combinations of the bosonic operators ϕ_l that enter the standard electron tunneling Lagrangian of the two contacts,

$$\mathcal{L}_t = \sum_{j=1,2} [T_j \psi_1^\dagger \psi_2|_{x=x_j} + \text{H.c.}]$$

can be expressed as the values at points $x_{1,2}$ of the same right-propagating chiral bosonic field

$$\phi_{-}(x) = \frac{\sqrt{\nu_1}\phi_0 - \sqrt{\nu_0}\phi_1}{\sqrt{\nu_0 + \nu_1}}. \quad (1)$$

The tunnel Lagrangian describing electron tunneling in the two contacts can then be written as

$$\mathcal{L}_t = \sum_{j=1,2} (DU_j/\pi) \cos[\lambda\phi_{-}(x_j) + \kappa_j], \quad (2)$$

where U_j and κ_j are the absolute values and the phases of the dimensionless tunneling amplitudes, $U_j e^{i\kappa_j} = T_j D/v$. The products of the Majorana fermions $\xi_1 \xi_2$ were omitted from Lagrangian (2), since they cancel out in each perturbative order due to charge conservation. The phases κ_j are obtained, as usual, by integrating the gauge-invariant phase of the electron operators along the two edges between the contacts. The phase difference includes then the contributions from the external magnetic flux Φ_{ex} and from the average electron numbers $N_{0,1}$ (which set the Fermi wave vectors) on the two sides of the interferometer

$$\kappa_2 - \kappa_1 = 2\pi[(\Phi_{ex}/\Phi_0) + (N_0/\nu_0) - (N_1/\nu_1)] + \text{const} \equiv -\kappa.$$

The factor $\lambda = \sqrt{2m}$ in Lagrangian (2) follows from the normalization of the bosonic field ϕ_{-} , which in the absence of tunneling is a free right-propagating chiral field. This field undergoes successive scattering at the two contacts by the tunneling terms of the Lagrangian. The scattering breaks the charge conservation and therefore creates tunneling current. The applied voltage can be introduced at first as a shift of the incoming field of one of the edges: $\phi_0 - \sqrt{\nu_0}Vt$. As one can see from Eq. (1), such a shift translates into the shift of the tunneling field $\phi_{-} - Vt/\lambda$.

The thermodynamic Bethe ansatz solution of the tunneling model was developed²² for a single-point tunneling contact with $\lambda^2 = 2m$ by application of one-particle boundary S matrices²³ to a distribution of the bosonic field excitations [kinks (+), antikinks (-), and $m-2$ sorts of breathers (b)], which were introduced through the massless limit of the ‘‘bulk’’ sine-Gordon model. The height of the kinks (antikinks) defined by the sine-Gordon interaction is equal to $\pi\lambda$. Therefore, as follows from Eq. (1), they carry charge $\pm e/2$ along the edges 0 and 1, respectively, while the breathers are neutral. This solution was generalized⁸ to the two tunneling contacts relevant for the MZI problem. Based on the chiral dynamics of the local fluctuations of the field $\phi_{-}(x)$, it has been argued that the quasiparticle scattering at the two point contacts occurs successively and independently at different points and, hence, is described by the successive application of two boundary S matrices to the same distribution of the excitations of the model. Since there is no kink(antikink)-breather transitions at the contacts, ($S_{j,k}^{b\pm} = 0$, $j=1,2$), only the kink-antikink (and vice versa) transitions are important for the charge transport, and their boundary S matrices conserving the quasiparticles momentum k (always positive for chiral propagation) are written as

$$S_{j,k}^{\pm\pm} = \frac{(ak/T_{jB})^{m-1} e^{i\alpha_k}}{1 + i(ak/T_{jB})^{m-1}}, \quad S_{j,k}^{\mp+} = \frac{e^{i(\alpha_k - \kappa_j)}}{1 + i(ak/T_{jB})^{m-1}}. \quad (3)$$

Here the standard energy scales T_{jB} are used to characterize the tunneling strength at the individual contacts, and

$$a = v \frac{2\sqrt{\pi}\Gamma(1/[2(1-\nu)])}{\nu\Gamma(\nu/[2(1-\nu)])}.$$

The explicit relation between the energy scales T_{jB} and electron tunneling amplitudes is given below.

III. CUMULANT-GENERATING FUNCTION FOR THE CHARGE TRANSFER DISTRIBUTION

At zero temperature, dynamics of the liquid should be described with only one type of quasiparticles, e.g., kinks, which fill out all available states with the bulk distribution $\rho(k)$, with k being the quasiparticle momentum, up to some limiting momentum A defined by the applied voltage. Each momentum- k quasiparticle undergoes successive scattering at the two tunneling contacts independently of other quasiparticles. The overall scattering process is described by the product of the two boundary S matrices given by Eq. (3). Our goal is to find the cumulant-generating function $\ln P(\xi)$ of the charge transfer between the two branches of the interferometer, which is defined, as usual, as the logarithm of the Fourier transform of the probability distribution function of the transferred charge. We measure the charge in units of the electron charge by setting $e=1$. Independence of the scattering events of quasiparticles with different momenta implies then that $\ln P(\xi)$ can be found as a sum of logarithm of the generating functions of individual momentum states, and its long-time asymptotics is

$$\ln P(\xi) = tv \int_0^A dk \rho(k) \ln p(k, \xi). \quad (4)$$

The generating function of one state with momentum k

$$p(k, \xi) = 1 + \tau_C(k)(e^{i\xi} - 1) \quad (5)$$

is defined by the total transition probability $\tau_C(k)$ of the momentum- k kink into antikink. Taking the product of the scattering matrices of the two contacts to find the total scattering matrix $\hat{S}_2 \hat{S}_1$, and using the parametrization of the contact tunneling strengths as $(T_{jB}/a)^2 \equiv \exp\{\theta_j/(m-1)\}$, we can write the probability $\tau_C(k)$ from the corresponding matrix element of $\hat{S}_2 \hat{S}_1$ as

$$\tau_C(k) = |(\hat{S}_2 \hat{S}_1)^{-+}|^2 = B[\tau(\theta_2, k) - \tau(\theta_1, k)]. \quad (6)$$

Here $\tau(\theta_j, k)$ are the transition probabilities in the individual point contacts

$$\tau(\theta_j, k) = |\hat{S}_j^{-+}|^2 = [1 + k^{2(m-1)} e^{-\theta_j}]^{-1}, \quad (7)$$

and the factor B characterizes interference between the two contacts

$$B(T_{jB}, \kappa) = \frac{|T_{1B}^{m-1} + T_{2B}^{m-1} e^{i\kappa}|^2}{T_{2B}^{2(m-1)} - T_{1B}^{2(m-1)}}. \quad (8)$$

Without a loss of generality, we assume below a specific relation between the tunneling strength parameters of the two contacts, $\theta_2 \geq \theta_1$, and write them as $\theta_{1,2} = \bar{\theta} \mp \Delta\theta_0$, with $\Delta\theta_0 \geq 0$.

The aim of our subsequent derivation is to find the cumulant-generating function $\ln P(\xi)$ in terms of the two generating functions $\ln P_S$ for charge transfer in an individual point contact that was found from the Bethe ansatz solution by Saleur and Weiss.²¹ This derivation does not need the explicit expressions for $\rho(k)$ and A which can be found in Ref. 22. Following the approach for one contact, we first relate $\ln P(\xi)$ in Eq. (4) to the effective tunneling current. To do this, we introduce the generalized tunneling probability $\tau_C(u, k)$

$$\tau_C(u, k) \equiv \{1 + [\tau_C^{-1}(k) - 1]e^{-u}\}^{-1}. \quad (9)$$

which is the solution of the following differential equation in the new parameter u :

$$\partial_u \tau_C(u, k) = [1 - \tau_C(u, k)]\tau_C(u, k) \quad (10)$$

that satisfies the initial condition $\tau_C(u, k)|_{u=0} = \tau_C(k)$. One can extend Eq. (5) for p to include the parameter u through the substitution $\tau_C(k) \rightarrow \tau_C(u, k)$. Equation (9) shows then that the logarithm of p extended this way can be expressed as

$$\ln p = \ln[1 + \tau_C(k)(e^{u+z} - 1)]|_{z=0}^{z=i\xi}. \quad (11)$$

Calculating the derivatives of Eq. (11) with respect to u and ξ , and using Eq. (9), one can see that

$$-i\partial_\xi \ln p = \partial_u \ln p + \tau_C(u, k) = \tau_C(u + i\xi, k). \quad (12)$$

Combining Eq. (12) with Eq. (4) in which p is extended to include the parameter u , one sees that the cumulant-generating function satisfies the following relation

$$\partial_{i\xi} \ln P(u, \xi)/t = \int_0^A k\rho(k)\tau_C(u + i\xi, k) \equiv I(u + i\xi, V), \quad (13)$$

which expresses it through the total tunneling current $I(u, V)$ in the two contacts that is defined by the generalized tunneling probability $\tau_C(u, k)$.

As the next step, one substitutes Eq. (6) into Eq. (9) and casts the total tunneling probability $\tau_C(u, k)$ into the following form

$$\tau_C(u, k) = B \frac{e^u \sinh \Delta\theta_0}{\sinh \Delta\theta(u)} \sum \pm \tau(\bar{\theta} \pm \Delta\theta(u), k), \quad (14)$$

where $\Delta\theta(u)$ is defined by the conditions that

$$\cosh \Delta\theta(u) = \cosh \Delta\theta_0 + B(e^u - 1)\sinh \Delta\theta_0 \quad (15)$$

and $\Delta\theta(u) > 0$. Differentiation of Eq. (15) shows that the coefficient in Eq. (14) in front of the sum can be written as the derivative of $\Delta\theta(u)$

$$\partial_u \Delta\theta(u) = B \frac{e^u \sinh \Delta\theta_0}{\sinh \Delta\theta(u)}. \quad (16)$$

Using Eqs. (14) and (16) in the definition of the tunneling current $I(u, V)$ Eq. (13) we obtain an important relation

$$I(u, V) = \partial_u \Delta\theta(u) \sum_{\pm} \pm I_{1/m}(\bar{\theta} \mp \Delta\theta(u), V), \quad (17)$$

which expresses the derivative of the cumulant-generating function Eq. (13) for the charge transfer in a symmetric interferometer in terms of the tunneling current $I_{1/m}$ in one point contact between the two edges with the effective filling factor $\nu = 1/m$. The current in one contact has been calculated²² from the Bethe ansatz solution, and its tunneling conductance

$$G_{1/m}[V/T_B] = G_{1/m}[(V/a)e^{-\theta[2(m-1)]}] = I_{1/m}(\theta, V)/V$$

is given at zero temperature by a universal scaling function expressed in the form of the low- and high-voltage expansion series. Integrating Eq. (17) over u , and using the result in Eq. (13), we express the generating function $\ln P(\xi) = \ln P(u, \xi)|_{u=0}$ in the following form:

$$\ln P(\xi) = -Vt \left\{ \int_{\theta_1}^{\bar{\theta} - \Delta\theta(i\xi)} + \int_{\theta_2}^{\bar{\theta} + \Delta\theta(i\xi)} \right\} d\theta \cdot G_{1/m}[(V/a)e^{-\theta[2(m-1)]}]. \quad (18)$$

The explicit expansion series for $G_{1/m}$ in Eq. (18) allow integration in each order. The integration transforms the generating function Eq. (18) into the sum of the two generating functions $\ln P_S$ for charge transfer in individual contacts and gives our key result

$$\ln P(\xi) = \sum_{j=1,2} \ln P_S(V/T_{jB}, e^{(-1)^j[\Delta\theta_0 - \Delta\theta(i\xi)]}). \quad (19)$$

The single-contact generating function $\ln P_S$ is known in terms of the low- and high-voltage expansion series²¹

$$\begin{aligned} \frac{\ln P_S(s, e^{i\xi})}{\sigma_0 V t} &= \sum_{n=1}^{\infty} \frac{c_n(m)}{mn} s^{2n(1/\nu-1)} (e^{in\xi} - 1), \quad s < e^\Delta \\ &= i\nu\xi + \sum_{n=1}^{\infty} \frac{c_n(\nu)}{n} s^{2n(\nu-1)} (e^{-in\nu\xi} - 1), \quad s > e^\Delta, \\ c_n(\nu) &= (-1)^{n+1} \frac{\Gamma(\nu n + 1)\Gamma(3/2)}{\Gamma(n+1)\Gamma[3/2 + (\nu-1)n]}, \end{aligned} \quad (20)$$

where

$$e^\Delta = (\sqrt{\nu})^{\nu(1-\nu)} \sqrt{1-\nu},$$

and σ_0 is the conductance quantum.

Equation (19) representing the total generating function $\ln P$ as the sum of the two single-contact generating functions $\ln P_S$ seems to suggest that the charge transfer in the MZI is divided into two independent processes associated with the two point contacts of the MZI. Indeed, one mani-

festation of this division is that the dependence of each of these processes on the bias voltage V (through the function P_S) is determined, as in Eq. (20), only by the characteristic energy scale T_{jB} of the corresponding junction. Also, similarly to the individual $\ln P_S$, the total generating function exhibits the transition from tunneling of integer electrons at low voltages to tunneling of the fractionally charged quasiparticles at large voltages. The division into individual single-contact generating functions is, however, not complete. The total generating function $\ln P$ depends also on the charge dynamics in the interferometer as a whole, since each individual charge transfer process in one contact triggers multiple charge transfers involving interference between both contacts of the interferometer. Information about this charge dynamics enters Eq. (19) through the function $\Delta\theta(u)$ determined by Eq. (15) and sensitive to both interferometer contacts. As discussed in more details below, one of the consequence of such interference is a relatively complex (non-Poisson) dynamics of quasiparticle tunneling at large voltages. This dynamics is created by the anyonic braiding statistics of the quasiparticles which gives a statistical contribution to the interference phase between the two contacts of the MZI that is changed by each quasiparticle tunneling. The interference can become irrelevant if the two contacts are strongly asymmetric. For $T_{2B} \gg T_{1B}$, the generating function $\ln P$ is well approximated at low voltages by the single-contact $\ln P_S$ defined by T_{1B} , i.e., by the strongest electron tunneling amplitude U_1 —see Eq. (24) below. At large voltages, the generating function $\ln P$ is approximated by the single-contact $\ln P_S$ defined by T_{2B} , i.e., by the weakest electron tunneling amplitude U_2 .

A. Low-voltage behavior of the generating function

At small voltages, when $V < T_{jB}e^\Delta$ for both $j=1,2$, the low-voltage expansions of the single-contact generating function $\ln P_S$ Eq. (20) for both terms in Eq. (19) can be combined as follows:

$$\ln P(\xi) = \sigma_0 V t \sum_{n=1}^{\infty} \frac{c_n(m)}{mn} \sum_{j=1,2} (V/T_{jB})^{2n(m-1)} \times \left\{ \frac{\cosh[n\Delta\theta(i\xi)]}{\cosh(n\Delta\theta_0)} - 1 \right\}. \quad (21)$$

Since $\cosh[n\Delta\theta(i\xi)]$ is a polynomial of $\cosh[\Delta\theta(i\xi)]$, and the latter, according to Eq. (15), is a linear function of $e^{i\xi}$, this expansion of the MZI generating function shows that at low voltages, the charge transfer between the edges of the MZI is quantized in units of electron charge.

More explicitly, using the standard expansion of $\cosh nx$ (see Eq. 1.331.4 in Ref. 24) and the relations that follow from Eqs. (8) and (15):

$$\cosh \Delta\theta(i\xi) = \cosh \Delta\theta_0 [1 + R(e^{i\xi} - 1)],$$

$$R \equiv B \tanh \Delta\theta_0 = \frac{|T_{1B}^{m-1} + T_{2B}^{m-1} e^{i\kappa}|^2}{T_{1B}^{2(m-1)} + T_{2B}^{2(m-1)}},$$

$$\cosh \Delta\theta_0 = \frac{T_{1B}^{2(m-1)} + T_{2B}^{2(m-1)}}{2(T_{1B}T_{2B})^{(m-1)}}, \quad (22)$$

we bring Eq. (21) into the following form:

$$\ln P(\xi) = \sigma_0 V t \sum_{n=1}^{\infty} \frac{c_n(m)}{mn} \left[\sum_j (V/T_{jB})^{2(m-1)} \right]^n \cdot \left\{ [1 + R(z-1)]^n + n \sum_{l=1}^{[n/2]} \frac{(-1)^l C_{l-1}^{n-l-1}}{l(2 \cosh \Delta\theta_0)^{2l}} \cdot [1 + R(z-1)]^{n-2l} \right\} \Big|_{z=1}^{z=e^{i\xi}}. \quad (23)$$

Equation (23) quantifies our previous conclusions about properties of the MZI charge transfer statistics Eq. (19) in the low-voltage regime. In the limit of strongly different contacts, $T_{2B} \gg T_{1B}$, one finds that $R \rightarrow 1$ and $\cosh \Delta\theta_0 \gg 1$ so that the charge transfer statistics Eq. (23) approaches that of one point contact²¹ characterized by T_{1B} (i.e., the strongest electron tunneling amplitude U_1) with corrections in T_{1B}/T_{2B} also quantized in the electron charge units. The n th term in the expansion of this statistics in powers of the bias voltage V corresponds in this case to tunneling of exactly n electrons. By contrast, the n th order term of the general MZI transfer statistics Eq. (23) involves transfer of all numbers of electrons up to n . In the lowest order in V , the MZI statistics reduces to the Poisson distribution, with the coefficient in front of $(z-1)$ in Eq. (23) equal to the average electron tunneling current. One can check this starting from Eq. (2) by direct perturbative calculation,⁸ if the energy scales T_{jB} are expressed through the electron tunneling amplitudes U_j

$$T_{jB} = 2D[\Gamma(m)/U_j]^{1/(m-1)}. \quad (24)$$

B. Large-voltage behavior of the generating function

At large voltages, $V > T_{jB}e^\Delta$, the combination large-voltage expansions of both single-contact generating functions $\ln P_S$ in Eq. (19) brings the total MZI generating function into the following form:

$$\ln P(\xi) = \sigma_0 V t \sum_{n=1}^{\infty} \frac{c_n(1/m)}{n} \sum_j (V/T_{jB})^{2n(1-m)/m} \times \left[\frac{\cosh(n\Delta\theta(i\xi)/m)}{\cosh(n\Delta\theta_0/m)} - 1 \right]. \quad (25)$$

In terms of the parameters introduced in Eq. (22), this equation can be rewritten as

$$\ln P(\xi) = \sigma_0 V t \sum_{n=1}^{\infty} \frac{c_n(1/m)}{n 2^{n/m}} \left[\sum_j (T_{jB}/V)^{2(m-1)} \right]^{n/m} \times \sum_{\pm} [1 + R(z-1) \pm ([1 + R(z-1)]^2 - \cosh^{-2} \Delta\theta_0)^{1/2}]^{n/m} \Big|_{z=1}^{z=e^{i\xi}}. \quad (26)$$

We can see again that in the asymmetric limit, $T_{2B} \gg T_{1B}$,

when $R \rightarrow 1$ and $\cosh \Delta \theta_0 \gg 1$, Eq. (26) for the charge transfer statistics reduces to that of a single point contact.²¹ The dominant contact is now characterized by the larger quasiparticle tunneling amplitude W_2 (i.e., smaller electron tunneling amplitude U_2) and corresponding energy scale T_{2B} , related to W_2 as

$$T_{jB} = 2mD[W_j/\Gamma(1/m)]^{m/(m-1)}. \quad (27)$$

The n th order term in the expansion in Eq. (26) of the generating function corresponds to the transfer of the fractional charge n/m by n quasiparticles. One can see, however, that the MZI transfer statistics Eq. (26) does not contain in general the terms $e^{i\xi/m}$ that would correspond directly to transfer of individual quasiparticles of charge $1/m$. In particular, the $n=1$ term of the expansion that gives the leading large-voltage contribution to the statistics, cannot be interpreted as a Poisson process of tunneling of independent quasiparticles, in contrast to the leading low-voltage term that did represent Poisson process of individual electron tunneling events. The reason for this is the m -state dynamics of the effective flux through the interferometer associated with the quasiparticle tunneling, which introduces correlations in the tunneling process. These correlations stem from the anyonic braiding statistics of the quasiparticles, with each tunneling quasiparticle changing the tunneling rate for the next quasiparticle by changing the statistical contribution to the effective interference phase between the two contacts of the interferometer. They can be most easily understood in the description of the quasiparticle tunneling based on the kinetic equation discussed in the next section.

IV. KINETIC EQUATION FOR THE LARGE-VOLTAGE CHARGE TRANSFER

To derive kinetic equation that reproduces the large-voltage asymptotics of the generating function Eq. (25), and therefore provides a simple physical picture of the dynamics of quasiparticle tunneling, we start by rewriting this asymptotics in terms of the quasiparticle tunneling amplitudes W_j . From the last relation in Eq. (22), we have

$$\cosh(\Delta \theta_0/m) = \frac{1}{2} \left[\left(\frac{T_{1B}}{T_{2B}} \right)^{(m-1)/m} + \left(\frac{T_{2B}}{T_{1B}} \right)^{(m-1)/m} \right]. \quad (28)$$

Using this equation to transform the leading, $n=1$, term in Eq. (25), and replacing the energy scales T_{jB} by the quasiparticle amplitudes W_j with the help of Eq. (27), we have

$$\ln P(z) = tK(V) \left[2W_1W_2 \cosh\left(\frac{\Delta \theta(z)}{m}\right) - \sum_j W_j^2 \right], \quad (29)$$

where $K(V) = \sigma_0 V (2mD/V)^{2(m-1)/m} c_1 (1/m) / \Gamma^2(1/m)$.

Kinetic equation describing the quasiparticle tunneling can be written down based on the following considerations. The general picture of the quasiparticle dynamics in the MZI discussed in the Introduction implies that the quasiparticles create statistical contribution to the effective flux through the interferometer. Because of this statistical contribution, the MZI can be found in m separate states which differ by the effective flux, with each tunneling quasiparticle changing

successively the state l into $l-1$ modulo m . Since the total rates of the quasiparticle tunneling in the MZI depend on the effective flux, such dynamics of flux introduces correlations into quasiparticle transitions, separating naturally the processes of successive quasiparticle tunneling events into the groups of m transitions. As usual, to cast the kinetic equation governing this flux dynamics into the form appropriate for the calculation of the cumulant-generating function, we multiply transition probabilities by a factor $z^{l/m} = e^{i\xi/m}$ that keeps track of the transferred charge. Then, we introduce the probabilities $d_{l,n}(t)$ that at time t the MZI is in the state l and n quasiparticles have been transferred through it. Combining these probabilities into an m -dimensional vector $Q_l(z, t) = \sum_n d_{l,n}(t) z^{n/m}$, one can write the kinetic equation in the following matrix form:

$$\partial_t Q_l(z, t) = \sum_{l'} M(z)_{l,l'} Q_{l'}(z, t). \quad (30)$$

According to the qualitative picture of quasiparticle tunneling discussed above, the transition matrix has a simple form, with the only nonvanishing elements are those on the main diagonal, $l=l'$, and those with $l=l'-1$

$$M(z)_{l,l'} = -\gamma_l \delta_{l,l'} + \gamma_{l'} z^{1/m} \delta_{l,l'-1}. \quad (31)$$

Here the Kronecker symbol $\delta_{l,l'}$ is defined modulo m . The leading large-time asymptotics of the generating function for the probability distribution evolving according to the kinetic equation (30) is (see, e.g., Ref. 25): $\ln P(z) = t\Lambda$, where Λ is the maximum eigenvalue of the transition matrix Eq. (31). The structure of this matrix shows directly that the characteristic equation $\det(M - \Lambda) = 0$ has the form

$$\prod_{l=0}^{m-1} (\gamma_l + \Lambda) - z \sum_{l=0}^{m-1} \gamma_l = 0. \quad (32)$$

The maximum eigenvalue Λ is the solution of this equation which goes to zero when $z \rightarrow 1$, since all other eigenvalues of the matrix $M(z=1)$ are negative.

Before trying to establish the general relation between the generating function obtained from this equation and the generating function Eq. (29), we consider the simple case $m=2$. In this case, Eq. (29) for the large-voltage asymptotics of the generating function Eq. (25), can be simplified further. First, we have from Eq. (22)

$$\cosh\left(\frac{\Delta \theta(z)}{2}\right) = \left[\cosh^2\left(\frac{\Delta \theta_0}{2}\right) + \frac{R}{2}(z-1) \cosh \Delta \theta_0 \right]^{1/2}.$$

Using this relation, Eq. (22), and Eq. (28) with $m=2$, we transform Eq. (29) into

$$\ln P(z) = tK(V) \left\{ \left[\left(\sum_j W_j^2 \right)^2 + |W_1^2 + W_2^2 e^{i\kappa}|^2 \cdot (z-1) \right]^{1/2} - \sum_j W_j^2 \right\}. \quad (33)$$

On the other hand, in the kinetic-equation approach, Eq. (32) be solved readily for $m=2$ giving the following expression for Λ :

$$\Lambda = \left[\left(\sum_j \gamma_j \right)^2 + 4\gamma_0\gamma_1(z-1) \right]^{1/2} - \sum_j \gamma_j / 2. \quad (34)$$

This equation describes the generating function for the statistics of any transfer process consisting of the two steps with the rates $\gamma_{0,1}$, e.g., incoherent charge transfer through a resonant level.²⁵ Comparison of Eqs. (33) and (34) shows that the generating function Eq. (34) obtained from the kinetic equation reproduces the large-voltage asymptotics Eq. (33) of the generating function Eq. (25), if the tunneling rates are taken as

$$\gamma_{0,1} = K(V)|W_1 + W_2 e^{i\phi_{0,1}}|^2, \quad \phi_l = (\kappa + \pi)/2 + \pi l. \quad (35)$$

Equation (35) for the tunneling rates agrees with the physical picture of quasiparticle tunneling discussed above. Statistical contribution to the effective flux through the MZI means that tunneling of each quasiparticle changes the phase between the interferometer contacts by $2\pi/m = \pi$ in agreement with the quasiparticle anyonic exchange statistics. Equation (35) also shows that the quasiparticles see a phase shift $\pi/2$ in addition to the phase $\kappa/2$ induced by the external magnetic flux. The origin of this phase shift is discussed below.

Following this logic, we look for solution of Eq. (32) in the case of arbitrary m taking the tunneling rates γ_l as

$$\gamma_l = K(V)|W_1 + W_2 e^{i\phi_l}|^2, \quad \phi_l = \phi + 2\pi l/m \quad (36)$$

with some unknown ϕ . With these tunneling rates, Eq. (32) reads

$$\prod_{l=0}^{m-1} \left(\cos \phi_l + \frac{\lambda + W_1^2 + W_2^2}{2W_1W_2} \right) = z \prod_{l=0}^{m-1} \frac{\gamma_l}{2K(V)W_1W_2}, \quad (37)$$

where $\lambda \equiv \Lambda/K(V)$. To further transform Eq. (37), we use the basic identity

$$x^m - 1 = \prod_{l=0}^{m-1} (x - e^{i2\pi l/m}), \quad (38)$$

and the two identities that follow directly from it

$$\prod_{l=0}^{m-1} 2 \cos \frac{\phi_l}{2} = 2 \cos \left(\frac{\phi}{2} m + \pi \frac{m-1}{2} \right),$$

$$2^{m-1} \prod_{l=0}^{m-1} \left[\cos \phi_l + \cosh \left(\frac{\Delta\theta}{m} \right) \right] = \cosh \Delta\theta - (-)^m \cos(m\phi). \quad (39)$$

The first one is obtained essentially by taking $x = -e^{i\phi}$ in Eq. (38), while the second one follows from the first if the sum of the cosines is transformed into their product. By direct comparison of the second identity in Eq. (39) with Eq. (37) we see that Λ as defined by $\ln P(z)/t$ in Eq. (29) indeed solves Eq. (32) if

$$\cosh \Delta\theta = (-)^m \cos(m\phi) + \frac{z}{2} \prod_{l=0}^{m-1} \frac{\gamma_l}{K(V)W_1W_2}. \quad (40)$$

Making use of Eq. (38) one more time, we calculate the product on the right-hand side of Eq. (40)

$$\prod_{l=0}^{m-1} \frac{\gamma_l}{K(V)W_1W_2} = \frac{|W_2^m e^{im(\phi-\pi)} - W_1^m|^2}{W_1^m W_2^m}. \quad (41)$$

One can see that with this expression for the product, Eq. (40) precisely coincides with the definition of $\cosh \Delta\theta(z)$ by Eq. (22). Indeed, combining all three relations in Eq. (22) one can express $\cosh \Delta\theta(z)$ as

$$\cosh \Delta\theta(z) = -\cos \kappa + \frac{|T_{1B}^{m-1} + T_{2B}^{m-1} e^{i\kappa}|^2}{2(T_{2B}T_{1B})^{(m-1)}} z. \quad (42)$$

Replacing T_{jB} in Eq. (42) with the amplitudes W_j through Eq. (27), we see that Eq. (42) precisely coincides with Eqs. (40) and (41), if $\cos \kappa = (-)^{(m+1)} \cos(m\phi)$, i.e., if the phase ϕ is chosen to satisfy the condition

$$m\phi = \kappa + (m-1)\pi. \quad (43)$$

The deviation of the phase ϕ from κ/m in this equation is important only for even m . In this case, it produces the shift $(m-1)\pi/m$ of the interference phase in the quasiparticle tunneling rates from the value induced by the external magnetic field. This shift coincides with the phase acquired by one of the two Klein factors of the MZI quasiparticle tunneling action of the MZI (Ref. 17) in the flux-diagonal representation due to the m -power periodicity condition for the Klein factors, which corresponds physically to the requirement of the proper exchange statistics between electrons and quasiparticles. This phase shift ensures, actually, that there is no shift in the interference pattern of the tunnel current in the interferometer (see the final results below) between the regimes of electron and quasiparticle tunneling.

V. CUMULANTS OF THE CHARGE TRANSFER DISTRIBUTION

So far, we have established the interpretation of the low- and high-voltage asymptotic behavior of the charge transfer statistics in terms of, respectively, tunneling of individual electrons and quasiparticles. In this section, we calculate the charge transfer cumulants in these two limits, with the emphasis on the quasiparticle limit which exhibits the nontrivial behavior of the cumulants. We also will use the generating function found in Sec. III for arbitrary voltages to calculate the full voltage dependence of the cumulants, and to study the crossover between the two asymptotic regimes of electron and quasiparticle tunneling. The cumulants of the charge $N(t)$ transferred through the interferometer during a large time interval t can be found from the cumulant-generating function Eq. (13) by the standard relation

$$\langle N^j(t) \rangle_c / t = \partial_u^j \ln P|_{u=0} / t = \partial_u^{j-1} I(u, V)|_{u=0}, \quad (44)$$

where the current $I(u, V)$ is given by Eq. (17).

The first cumulant gives the average tunneling current: $I(V) \equiv I(0, V) = \langle N(t) \rangle / t$. At arbitrary voltages, the average current was calculated before in Ref. 17. Its large- V asymptotics can also be obtained directly from Eqs. (26) and (27)

$$I(V) = \frac{K(V)}{m} B(W_2^2 - W_1^2) = \frac{1}{\sum_l \gamma_l^{-1}}, \quad (45)$$

where the interference factor B Eq. (8) can be expressed in term of the quasiparticle amplitudes $W_{1,2}$ as

$$B(W_j, \kappa) = \frac{|W_1^m + W_2^m e^{i\kappa}|^2}{W_2^{2m} - W_1^{2m}}. \quad (46)$$

The second equality in Eq. (45) provides direct interpretation of the asymptotics of the average current in terms of the quasiparticles transitions.⁷ It can be proven formally by making use of the identity

$$\sum_l \gamma_l^{-1} = \frac{W_1 \partial_{W_1} - W_2 \partial_{W_2}}{2K(V)(W_1^2 - W_2^2)} \ln \left[\prod_l \gamma_l \right], \quad (47)$$

which can be obtained by directly differentiating individual rates γ_l in this equation. On the other hand, differentiating the product of all γ_l 's together, as given by Eq. (41), and using Eq. (43), we obtained the second equality in Eq. (45). This equality agrees naturally with the simple solution of the quasiparticle kinetic equation, which gives the average tunneling rate as inverse of the average tunneling times in the different states of the interferometer.

The second cumulant $\langle N^2(t) \rangle$ defines the spectral density of the current fluctuations at zero frequency $S_I(0) = \langle N^2(t) \rangle_c / t$, which at zero temperature reflects the shot noise associated with the charge transfer processes. From Eq. (17), one can write the first derivative of the current as

$$\begin{aligned} \partial_u I(u, V) &= I(u, V) \times \partial_u \ln [\partial_u \Delta \theta(u)] \\ &\quad - [\partial_u \Delta \theta(u)]^2 \sum_{\pm} \partial_{\bar{\theta}} I_{1/m}(\bar{\theta} \mp \Delta \theta(u), V). \end{aligned} \quad (48)$$

Substituting this formula into Eq. (44) and calculating the derivatives of $\Delta \theta(u)$ Eq. (16) for $u \rightarrow 0$ we obtain expression for the spectral density of current

$$S_I(0) = (1 - B \coth \Delta \theta_0) I - B^2 \sum_{j=1,2} \partial_{\theta} I_{1/m}(\theta_j, V). \quad (49)$$

It is convenient to characterize the shot noise represented by this spectral density through the Fano factor F defined as $F = S_I(0)/I$. In the case of MZI, the Fano factor reflects both the charge and statistics of the tunneling excitations and illustrates the transition between the electron and quasiparticle regimes. In the low-voltage limit, $F=1$ as a result of the regular Poisson process of electron tunneling. To find the Fano factor in the quasiparticle, large-voltage, limit, we start with Eq. (49) which gives the following general expression for F :

$$\begin{aligned} F &= 1 - B \left\{ \coth \Delta \theta_0 - \sum_j \partial_{\theta} I_{1/m}(\theta_j, V) \right. \\ &\quad \left. \times \left[\sum_j (-1)^j I_{1/m}(\theta_j, V) \right]^{-1} \right\}. \end{aligned} \quad (50)$$

Using Eq. (22), the fact that in the large-voltage limit only one quasiparticle tunneling term $\propto W^2$ can be kept in the current $I_{1/m}$, cf. Eq. (45), and that with the parametrization of

the energy scales T_{jB} with θ introduced above, $W^2 \propto e^{\theta/m}$, we get from Eq. (50)

$$F = 1 - B \left\{ \frac{W_2^{2m} + W_1^{2m}}{W_2^{2m} - W_1^{2m}} - \frac{1}{m} \frac{W_2^2 + W_1^2}{W_2^2 - W_1^2} \right\}. \quad (51)$$

The Fano factor Eq. (51) corresponds to the dynamics of quasiparticle tunneling as described by the kinetic Eq. (30). This can be seen by following the steps similar to that taken above for the average current. Applying the differential operator from Eq. (47) to individual terms in the sum of the inverse tunneling rates γ_l , one obtains directly the following identity:

$$-\frac{W_1 \partial_{W_1} - W_2 \partial_{W_2}}{2K(V)(W_1^2 - W_2^2)} \sum_l \gamma_l^{-1} = \sum_l \gamma_l^{-2}.$$

On the other hand, replacing the sum of inverse γ_l 's in this equation with the corresponding expression from Eq. (45)

$$\sum_l \gamma_l^{-1} = m/[BK(V)(W_2^2 - W_1^2)],$$

and performing differentiation, we see that the large-voltage asymptotics Eq. (51) of the Fano factor can be written in terms of the tunneling rates γ_l as

$$F = \sum_l \gamma_l^{-2} / \left(\sum_l \gamma_l^{-1} \right)^2.$$

This result agrees with the calculation²⁶ based directly on the kinetic equation. Because of the complex nature of the quasiparticle tunneling dynamics characterized by m different tunneling rates γ_l , F is not equal simply to the quasiparticle charge $1/m$ but varies as a function of parameters, e.g., the interference phase κ , between $1/m$ and 1.

At arbitrary bias voltage V , the Fano factor F should be plotted numerically. Figure 2 shows F in the case $m=3$ which corresponds, e.g., to tunneling between the two $\nu=1/3$ edges. The curves are shown for different degrees of asymmetry between the two contacts of the interferometer and two values of interference phase, maximum constructive interference, $\kappa=0$, and complete destructive interference, $\kappa=\pi$. The range of variation of F with the interference phase κ decreases with increasing junction asymmetry. In general, the curves show the transition between electron tunneling with $F=1$ at small voltages V to quasiparticle tunneling at large voltages. In the quasiparticle regime, F is still can be significantly different from $1/3$ because of the nontrivial three-state flux dynamics of the MZI. In particular, for identical junctions, the three total quasiparticle tunneling rates in Eq. (36) satisfy the relation: $\gamma_l \propto \cos^2(\phi_l/2)$. Taking into account Eq. (43) for the nonstatistical contribution to the interference phase, one can see that under the condition of destructive interference, $\kappa \approx \pi$, the tunneling rate in one of the flux states of the interferometer, $l=0$, is much smaller than the rates in the two other states. This mean that on the relevant large time scale set by the smallest rate, the three quasiparticles transition that transfer interferometer from state $l=0$ back to itself happen almost simultaneously, so that the three quasiparticle charges $1/3$ are effectively transferred together, restoring F back to 1. Away from the regime of com-

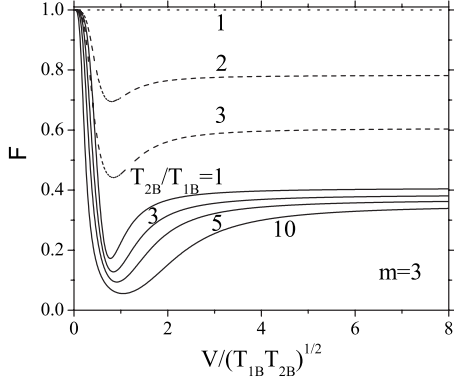


FIG. 2. The zero-temperature Fano factor F of the tunnel current in the Mach-Zehnder interferometer formed by two $\nu=1/3$ edges, i.e., for $m=3$, as a function of the bias voltage V for different degrees of asymmetry of the tunneling strength of the two contacts characterized by the T_{1B}/T_{2B} ratio. The solid curves corresponds to the case of complete constructive interference, $\kappa=0$; for the dashed curves, $\kappa=\pi$. In the latter case, $F=1$ identically for identical contacts, $T_{1B}/T_{2B}=1$. The curves illustrate the transition between the electron regime $F=1$ at small voltages to the quasiparticle m -state tunneling dynamics at large voltages. The transition region is characterized by the Fano factor F reaching the minimum below the quasiparticle minimum $1/m=1/3$.

plete destructive interference, there is a transition region between the electron and quasiparticle tunneling which is characterized by the Fano factor F reaching the minimum below the quasiparticle minimum $1/m=1/3$. With increasing junction asymmetry, the minimal value decreases, while the minimum becomes broader and moves to large voltages. This behavior is qualitatively independent of m , see Fig. 3 below for $m=2$.

Finally, we study the third charge transfer cumulant that characterizes the asymmetry around average of the transferred charge distribution, and has been measured experi-

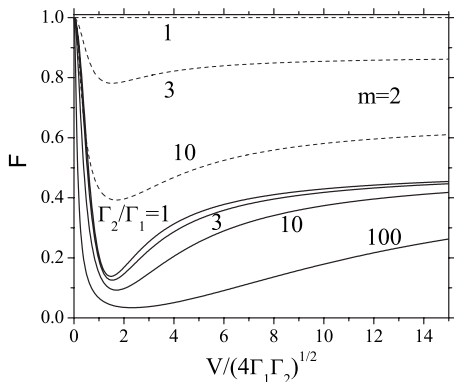


FIG. 3. The zero-temperature Fano factor F of the tunnel current for $m=2$, i.e., in the Mach-Zehnder interferometer formed by edges with $\nu=1/3$ and $\nu=1$, as given by Eq. (59). The solid curves corresponds to the case of complete constructive interference, $\kappa=0$; for the dashed curves, $\kappa=\pi$. In the latter case, $F=1$ identically for identical contacts. In general, the transition from the electron regime $F=1$ at small voltages to the two-state tunneling dynamics of quasiparticles at large voltages is characterized by the Fano factor F reaching the minimum in the crossover region.

mentally for electron tunneling in metallic tunnel junctions—see, e.g., Refs. 27 and 28 and in quantum point contacts.²⁹ As for the other cumulants, the large-time asymptotic of the third cumulant is linear in time, and it can be characterized by the coefficient $C_3 \equiv \langle N^3 \rangle_c / t$. To calculate this coefficient, we first find the second derivative of the tunnel current from Eq. (48)

$$\begin{aligned} \partial_u^2 I(u, V) &= \{ \partial_u^2 \ln \partial_u \Delta \theta(u) + [\partial_u \ln \partial_u \Delta \theta(u)]^2 \} I \\ &\quad - \sum_{\pm} [3 \partial_u \Delta \theta \partial_u^2 \Delta \theta \partial_{\theta} \mp (\partial_u \Delta \theta)^3 \partial_{\theta}^2] I_{1/m}(\bar{\theta} \mp \Delta \theta, V). \end{aligned} \quad (52)$$

Derivatives of $\Delta \theta(u)$ here can be found from Eq. (16). In particular, the coefficient in front of I in Eq. (52) can be expressed as

$$\begin{aligned} &\partial_u^2 \ln \partial_u \Delta \theta(u) + [\partial_u \ln \partial_u \Delta \theta(u)]^2 \\ &= 1 - 3 \coth \Delta \theta(u) \times \partial_u \Delta \theta(u) + [3 \coth^2 \Delta \theta(u) - 1] \\ &\quad \times [\partial_u \Delta \theta(u)]^2. \end{aligned} \quad (53)$$

Substitution of Eqs. (16), (52), and (53) into Eq. (44) gives us the coefficient C_3 of the third cumulant

$$\begin{aligned} C_3 &= [1 - 3B \coth \Delta \theta_0 + B^2(3 \coth^2 \Delta \theta_0 - 1)] I \\ &\quad - \sum_{j=1,2} [3B^2(1 - B \coth \Delta \theta_0) \partial_{\theta} I_{1/m}(\theta_j, V) \\ &\quad + (-)^j B^3 \partial_{\theta}^3 I_{1/m}(\theta_j, V)]. \end{aligned} \quad (54)$$

The ratio $F_3 = C_3/I$ has also been suggested³⁰ as a possible alternative to the Fano factor to characterize the charge of the tunneling particles. Indeed, in a Poisson process, F_3 is equal to the Fano factor multiplied by the tunneling charge. Therefore, in the case of MZI, F_3 Eq. (54) reduces to 1 in the low-voltage limit, as a result of the regular Poisson electron tunneling. In the quasiparticle, large-voltage, limit, repeating the calculation similar to that leading to Eq. (50), we can relate both factors as follows:

$$\begin{aligned} F_3 &= 3F - 2 + B^2 \left\{ 2 + \frac{1}{m^2} + \frac{12W_2^{2m}W_1^{2m}}{(W_2^{2m} - W_1^{2m})^2} \right. \\ &\quad \left. - \frac{3(W_2^2 + W_1^2)(W_2^{2m} + W_1^{2m})}{m(W_2^2 - W_1^2)(W_2^{2m} - W_1^{2m})} \right\}. \end{aligned} \quad (55)$$

VI. CHARGE TRANSFER STATISTICS FOR $m=2$

For general m , the results for the cumulants of the charge transfer statistics in the MZI discussed above could not be presented in a finite analytical form for arbitrary bias voltages. As we show in this section, the situation is simpler for $m=2$, when the kink quasiparticles of the bulk sine-Gordon model that provide the basis for the Bethe-ansatz solution of the MZI transport are the regular fermions (though carrying charge $1/2$), and their distribution $\rho(k)$ in Eq. (4) is the Fermi-Dirac step function. In practice, the $m=2$ regime should take place in the MZI formed by the two edges of different Quantum Hall liquids, with filling factors $\nu=1/3$ and $\nu=1$, i.e., $m_0=1$, $m_1=0$, and $m=1+m_0+m_1=2$. Indi-

vidual tunneling contacts of this type have been realized experimentally.¹⁹ Using the Fermi-Dirac property of the distribution function $\rho(k)$ for $m=2$, one can obtain the cumulant generating function $\ln P(\xi)$ either by integration in Eq. (4), or equivalently, by direct substitution into Eq. (18) of the known single-contact tunnel conductance $G_{1/2}$, which can be expressed simply as $G_{1/2}(s) = \sigma_0[1 - \arctan(2s)/(2s)]/2$. The resulting generating function is

$$\ln P(\xi) = \sigma_0 V t \sum_{j=1,2} \{y_j(u) \arctan[1/y_j(u)] + (1/2) \ln[1 + y_j^2(u)]\} \Big|_{u=0}^{u=i\xi}, \quad (56)$$

where $y_j(u) \equiv y_j(0) \exp\{(-1)^j [\Delta\theta(u) - \Delta\theta_0]/2\}$, and $y_j(0) \equiv T_{jB}/(2V)$.

This generating function can be combined with Eq. (44) to calculate the cumulants of the transferred charge distribution for $m=2$ using the same steps as in the previous section. Alternatively, one can substitute Eq. (4) into Eq. (44) and perform the integration directly. Below we briefly discuss the first three cumulants obtained in this way. The first cumulant gives the average tunneling current in the MZI as¹⁷

$$I = \sigma_0 B (\Gamma_2 I_2 - \Gamma_1 I_1), \quad (57)$$

where $I_j \equiv \arctan(V/2\Gamma_j)$, and $\Gamma_j \equiv T_{jB}/4 = DW_j^2/\pi$ are the characteristic quasiparticle tunneling rates in separate contacts. Using the fact that $K(V) = \sigma_0 D$ for $m=2$, one can see explicitly that the current agrees at large voltages with Eq. (45) that follows from the quasiparticle kinetic equation with the tunneling rates Eq. (35):

$$I = \frac{\pi\sigma_0}{2} \frac{|\Gamma_1 + \Gamma_2 e^{i\kappa}|^2}{\Gamma_1 + \Gamma_2} = \frac{\gamma_0 \gamma_1}{\gamma_0 + \gamma_1}. \quad (58)$$

It is interesting to note that this agreement relies strongly on the shift of the interference phase Eq. (43) from the externally induced phase κ .

The second cumulant gives the following expression for the Fano factor at arbitrary voltages, including the transition region between electron and quasiparticle tunneling:

$$F = 1 - \frac{|\Gamma_1 + \Gamma_2 e^{i\kappa}|^2}{\Gamma_1 I_1 - \Gamma_2 I_2} \left\{ \frac{2\Gamma_1 \Gamma_2 (\Gamma_2 I_1 - \Gamma_1 I_2)}{(\Gamma_1^2 - \Gamma_2^2)^2} + \frac{1}{2(\Gamma_1^2 - \Gamma_2^2)} \sum_{j=1,2} \Gamma_j \left[I_j + \frac{V/2\Gamma_j}{1 + (V/2\Gamma_j)^2} \right] \right\}. \quad (59)$$

This equation is plotted in Fig. 3 and describes the transition from $F=1$ for electron tunneling at small voltages to

$$F = 1 - \frac{1}{2} \frac{|\Gamma_1 + \Gamma_2 e^{i\kappa}|^2}{(\Gamma_1 + \Gamma_2)^2}$$

for quasiparticle tunneling at large voltages. One can see that the quasiparticle charge $e/2$ manifests itself most clearly for $\kappa=0$, when the total quasiparticle tunneling rates Eq. (35) coincide, $\gamma_1 = \gamma_2$, regardless of the relation between the individual rates Γ_j . Similarly to the case $m=3$ illustrated in Fig. 2, the Fano factor reduces to electron value 1 even in the quasiparticle regime, if $\Gamma_1 \approx \Gamma_2$ and $\kappa = \pi$. In this case, one of the total quasiparticle tunneling rates γ is much smaller than

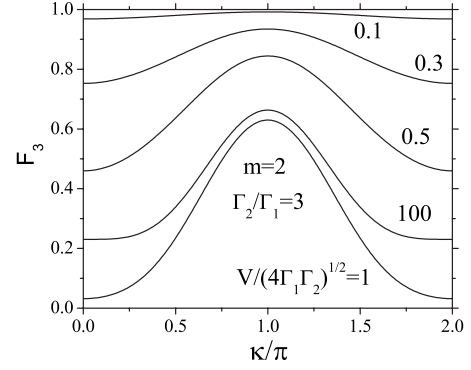


FIG. 4. Alternative “Fano factor” $F_3 = C_3/I$ Eq. (60) related to the third cumulant of the tunnel current noise in the Mach-Zehnder interferometer with $m=2$ and zero temperature, as a function of the interferometer phase κ . The curves are plotted for several bias voltages V between the interferometer edges and illustrate the transition between the electron and quasiparticles tunneling with increasing voltage. The transition is characterized by the nonmonotonous change in F_3 , which reaches minimum at the intermediate voltages.

the other, so on the relevant large time scale set by the smaller rate the quasiparticles effectively tunnel together, restoring F to 1.

Calculating the third cumulant, we find the following expression for the “alternative” Fano factor:

$$F_3 = 3F - 2 + \frac{|\Gamma_1 + \Gamma_2 e^{i\kappa}|^4}{4(\Gamma_1 I_1 - \Gamma_2 I_2)(\Gamma_1^2 - \Gamma_2^2)^2} \sum_{j=1,2} \times \left\{ (-1)^{j+1} \times \frac{3\Gamma_j I_j (\Gamma_j^4 + 10\Gamma_j^2 \Gamma_{j'}^2 + 5\Gamma_{j'}^4)}{(\Gamma_1^2 - \Gamma_2^2)^2} + \frac{3V}{2(\Gamma_1^2 - \Gamma_2^2)} \times \frac{\Gamma_j^2 + 3\Gamma_{j'}^2}{1 + (V/2\Gamma_j)^2} + (-1)^{j+1} \frac{V}{[1 + (V/2\Gamma_j)^2]^2} \right\}, \quad (60)$$

where j' is defined by $j, j' = 1, 2$, $j' \neq j$. Equation (60) is plotted in Fig. 4, which shows F_3 as a function of the interference phase κ at several voltages. Voltage dependence of F_3 is qualitatively very similar to that of the Fano factor shown in Fig. 3: it approaches 1 at small voltages, in agreement with the underlying Poisson tunneling process of electrons. At large voltages, Eq. (60) reduces to the following form:

$$F_3 = 3F - 2 + \frac{3}{4} \frac{|\Gamma_1 + \Gamma_2 e^{i\kappa}|^4}{(\Gamma_1 + \Gamma_2)^4}.$$

This expression can be understood in terms of the same two-state tunneling dynamics of the quasiparticles that was discussed above. Also similarly to the Fano factor, the voltage dependence of F_3 is nonmonotonic, with a minimum between the regimes of electron and quasiparticle tunneling. The main qualitative difference between the noise-related Fano factor and its third-cumulant alternative is that the minimum of F_3 can become negative for some values of parameters (regime not shown in Fig. 4).

VII. CONCLUSION

Starting from the exact solution of the tunneling model of symmetric Mach-Zender interferometer in the FQHE regime, we have calculated the statistics of the charge transfer between interferometer edges. The obtained statistics shows the transition from electron tunneling at low voltages to tunneling of anyonic quasiparticles of the fractional charge e/m and statistical angle π/m at large voltages. Deep in the electron tunneling regime, the dynamics of charge transfer is represented by the standard Poisson process. Dynamics of quasiparticle tunneling is more complicated and reflects the existence of m effective flux states of the interferometer. The interference phase between the quasiparticle tunneling amplitudes in two contacts of the interferometer contains a con-

tribution from the quasiparticle exchange statistics, making the quasiparticle tunneling rates in different interferometer states different. In general, the transition from electron to quasiparticle tunneling is reflected in the Fano factor F or its third-cumulant alternative F_3 , which both reach minima in the transition region. However, in the regime close to complete destructing interference (interferometer phase $\kappa=\pi$ and equal tunneling strength in the two contacts), both F and F_3 have electron value 1 for all voltages.

ACKNOWLEDGMENTS

V.V.P. acknowledges support of the ESF Science Program INSTANS and Grant No. PTDC/FIS/64926/2006 of FCT (Foundation for Science and Technology, Portugal).

-
- ¹Y. Ji, Y. Chung, D. Sprinzak, M. Heiblum, D. Mahalu, and H. Shtrikman, *Nature (London)* **422**, 415 (2003); I. Neder, M. Heiblum, Y. Levinson, D. Mahalu, and V. Umansky, *Phys. Rev. Lett.* **96**, 016804 (2006).
- ²L. V. Litvin, H.-P. Tranitz, W. Wegscheider, and C. Strunk, *Phys. Rev. B* **75**, 033315 (2007).
- ³P. Roulleau, F. Portier, D. C. Glattli, P. Roche, A. Cavanna, G. Faini, U. Gennser, and D. Mailly, *Phys. Rev. B* **76**, 161309(R) (2007).
- ⁴V. J. Goldman and B. Su, *Science* **267**, 1010 (1995).
- ⁵D. V. Averin and J. A. Nesteroff, *Phys. Rev. Lett.* **99**, 096801 (2007).
- ⁶C. L. Kane, *Phys. Rev. Lett.* **90**, 226802 (2003).
- ⁷K. T. Law, D. E. Feldman, and Y. Gefen, *Phys. Rev. B* **74**, 045319 (2006).
- ⁸V. V. Ponomarenko and D. V. Averin, *Phys. Rev. Lett.* **99**, 066803 (2007).
- ⁹L. Saminadayar, D. C. Glattli, Y. Jin, and B. Etienne, *Phys. Rev. Lett.* **79**, 2526 (1997).
- ¹⁰R. de-Picciotto, M. Reznikov, M. Heiblum, V. Umansky, G. Bunin, and D. Mahalu, *Nature (London)* **389**, 162 (1997).
- ¹¹D. V. Averin and V. J. Goldman, *Solid State Commun.* **121**, 25 (2001).
- ¹²S. Das Sarma, M. Freedman, and C. Nayak, *Phys. Rev. Lett.* **94**, 166802 (2005).
- ¹³A. Stern, *Ann. Phys.* **323**, 204 (2008).
- ¹⁴X. G. Wen, *Adv. Phys.* **44**, 405 (1995).
- ¹⁵T. Jonckheere, P. Devillard, A. Crepieux, and T. Martin, *Phys. Rev. B* **72**, 201305(R) (2005).
- ¹⁶I. Levkivskiy, J. Froehlich, and E. Sukhorukov, [arXiv:1005.5703](https://arxiv.org/abs/1005.5703) (unpublished).
- ¹⁷V. V. Ponomarenko and D. V. Averin, *Phys. Rev. B* **79**, 045303 (2009).
- ¹⁸V. V. Ponomarenko and D. V. Averin, *Phys. Rev. B* **71**, 241308(R) (2005).
- ¹⁹S. Roddaro, N. Paradiso, V. Pellegrini, G. Biasiol, L. Sorba, and F. Beltram, *Phys. Rev. Lett.* **103**, 016802 (2009).
- ²⁰L. S. Levitov and G. B. Lesovik, *JETP Lett.* **58**, 230 (1993).
- ²¹H. Saleur and U. Weiss, *Phys. Rev. B* **63**, 201302(R) (2001).
- ²²P. Fendley, A. W. W. Ludwig, and H. Saleur, *Phys. Rev. Lett.* **74**, 3005 (1995); *Phys. Rev. B* **52**, 8934 (1995).
- ²³S. Ghoshal and A. B. Zamolodchikov, *Int. J. Mod. Phys. A* **9**, 3841 (1994).
- ²⁴I. S. Gradshteyn and I. M. Ryzhik, *Table of Integrals, Series, and Products* (Academic Press, New York, 2007).
- ²⁵D. A. Bagrets and Yu. V. Nazarov, *Phys. Rev. B* **67**, 085316 (2003).
- ²⁶D. E. Feldman, Y. Gefen, A. Kitaev, K. T. Law, and A. Stern, *Phys. Rev. B* **76**, 085333 (2007).
- ²⁷A. V. Timofeev, M. Meschke, J. T. Peltonen, T. T. Heikkilä, and J. P. Pekola, *Phys. Rev. Lett.* **98**, 207001 (2007).
- ²⁸Q. Le Masne, H. Pothier, N. O. Birge, C. Urbina, and D. Esteve, *Phys. Rev. Lett.* **102**, 067002 (2009).
- ²⁹G. Gershon, Y. Bomze, E. V. Sukhorukov, and M. Reznikov, *Phys. Rev. Lett.* **101**, 016803 (2008).
- ³⁰L. S. Levitov and M. Reznikov, *Phys. Rev. B* **70**, 115305 (2004).